Materials & Design 266 (2026) 116116

Contents lists available at ScienceDirect

Materials & Design

journal homepage: www.elsevier.com/locate/matdes

Wetting and capillary driven crack self-healing in metals revealed through Al/Sn/Al thin film model architectures

Subisha Balakumar [a,*], Stanislav Mráz [a,*], Marcus Hans [a], Markus Momma [a], Leandro Tanure [b], Hauke Springer [c], Jochen M. Schneider [a,d]

[a] Materials Chemistry, RWTH Aachen University, Kopernikusstr. 10, 52074 Aachen, Germany
[b] Oxford Sigma, Summertown Pavilion, 18 - 24 Middle Way, Oxford OX2 7LG, United Kingdom
[c] Sustainable Metallurgy, Universität Duisburg Essen, Friedrich Ebert Strasse 12, 47119 Duisburg, Germany
[d] Max-Planck-Institute for Sustainable Materials GmbH, 40237 Düsseldorf, Germany

ARTICLE INFO

Keywords:
Aluminum
Tin
Damage
Self-healing
Wetting
Capillary force
Thin film model

ABSTRACT

Thermally-activated, liquid-based crack healing was investigated using a magnetron sputtered Al / Sn / Al thin film architecture as a model system for bulk healing, with Sn acting as the healing agent. A brittle Al_2O_3 layer was sputtered prior to the deposition of the Al and Sn layers, enabling the formation of cracks with varying widths in the Al layers (2–4 μm) using a 3-point bending technique. Thermal activation was achieved through annealing at 250°C for 10 min and 400°C for 10 and 30 min. Scanning transmission electron microscopy imaging revealed that Sn mobility was activated only after annealing at 400°C for 30 min, resulting in efficient healing of ~ 2 μm wide cracks, while > 3 μm wide cracks showed a reduced healing efficiency in comparison. The here observed variations in healing efficiency are governed by the temperature-dependent wetting behavior of Al by Sn, as well as by crack-width-dependent capillary forces and the healing time. This study provides insights into the fundamental mechanisms governing liquid-based self-healing in metals, contributing towards future knowledge-driven design of self-healing bulk metals and metallic thin films.

1. Introduction

From a sustainability perspective, limited lifespan of materials, owing to susceptibility to microscopic damage during manufacturing and/or application and its subsequent loss of functionality, is among the grand challenge to be tackled. Generally, metallic engineering parts exhibit substantial microscopic damage stemming from their manufacture, e.g., pores from casting or cracks from rolling, bending, or deep drawing that may affect their performance adversely [1,2]. While numerous studies are being carried out to improve the performance of metallic materials by utilizing various strengthening mechanisms, damage management is seldom studied [3]. In this context, self-healing materials have re-emerged as an increasingly important research direction in the field of sustainable materials engineering.

Drawing inspiration from self-healing observed in biological organisms, there is a growing interest in applying similar mechanisms to mitigate damage in man-made materials. Self-healing has been successfully incorporated in polymer materials due to their cross-chain bonding and low melting points, facilitating easier diffusion and reestablishment of bonds between their motifs [4–6]. However, achieving thermally-driven self-healing on a macroscopic scale in metals proves challenging due to stronger bonds and lower diffusion rates of atoms compared to polymers [7,8]. However, Danzi et al. demonstrated a rapid, room-temperature, on-demand healing concept for metal films using Ni/Al multilayers as heat source, eliminating the need for external annealing and enabling repair in temperature-sensitive electronic systems [9]. Furthermore, Trost et al. recently reported an autonomous intrinsic self-healing mechanism for metallic thin films based on segregation-stabilized metastable $Mo_{1-x}Ag_x$ systems, enabling low-temperature crack healing in flexible microelectronics [10].

Previous studies report three mechanisms to achieve self-healing in metals: precipitation [11–14], shape memory effect [15–18]and redistribution of a low-melting point healing agent [19–22]. Dynamic precipitation of solute atoms in underaged Al-Cu-Mg-Ag alloys was found to reduce the creep rate and cause crack closure under fatigue loading conditions [11,12]. Several studies have shown usage of shape memory alloy (SMA) wires being used as reinforcements [15–17]. When cracks are generated perpendicularly to the direction of reinforcement and are

* Corresponding authors.
E-mail address: balakumar@mch.rwth-aachen.de (S. Balakumar).

https://doi.org/10.1016/j.matdes.2026.116116
Received 1 August 2025; Received in revised form 7 April 2026; Accepted 24 April 2026
Available online 25 April 2026

heated to high temperatures to activate the shape memory effect, crack closure was observed [15–17].

In bulk metals, the incorporation of low melting point healing agents is typically accomplished by encapsulating them within ceramic hollow spheres or cylinders, which are subsequently embedded within the matrix metal. The self-healing mechanism operates by relying on damage that fractures the ceramic casing, subsequent heating to melt the healing agent and thereby releasing it into the crack. In one such system, self-healing within an Al-Cu matrix was studied by embedding ceramic hollow tubes filled with 40 wt% Pb and 60 wt% Sn solder [21]. After generating cracks in the samples, heating the samples to 300°C liquefied the solder, which flowed into the cracks causing healing. However, the interface between the solder and Al-Cu matrix exhibited poor adhesion leading to interfacial porosity. Similarly, self-healing in Al-based metal-matrix composites reinforced with hollow microspheres, containing low melting point metals such as Zn, Sn and Bi, was investigated experimentally and by computational fluid dynamics modeling [22]. The authors argued that systems with low contact angle between the healing agent and the matrix, i.e., with better wetting, showed efficient healing [22]. However, an issue in systems with ceramic casings containing healing agent is the tendency for cracking at the metal-ceramic interface rather than the casing itself, which would then hinder the flow of the healing agent, undermining the functionality of the system. Furthermore, this limitation compromises the mechanical integrity of the component, reducing the attractiveness for applications. A recent study investigated Al-40 wt% Sn as a composite phase change material (C-PCM) for thermal energy storage, focusing on the effect of self-healing heat treatments at 250°C for 1 h on samples with varying microstructures and Sn distributions. The authors suggest that while molten Sn mobility can aid in restoring thermal diffusivity by improving its material continuity, its effectiveness is highly dependent on microstructural stability and Sn distribution [23].

Previous studies on self-healing of bulk Al-Sn composites have investigated either the crack-filling mechanism when Sn was encapsulated in ceramic hollow spheres [22], the effect of crack filling by Sn on the restoration of thermal properties [23], or mechanical properties [24]. We previously demonstrated proof-of-concept for self-healing in a bulk Al-4.28 wt% Sn alloy, showing improved ductility in the healed condition compared to pure Al, supported by evidence of crack filling by Sn observed using thin film model systems [24]. However, the fundamental mechanisms that govern the crack filling behavior in the Al-Sn system, when Sn is directly in contact with the Al matrix, remain largely unexplored. This is precisely where thin film model systems prove valuable- during film synthesis, compositions and volume fractions of the constituent building blocks forming the thin film architecture can be controlled precisely. This control enables the breakdown of complex bulk healing phenomena into simpler, more well-defined processes, as demonstrated here, by adjusting the volume fractions of healing agent relative to the matrix to be healed. Additionally, the controlled introduction and isolation of small-scale damage is readily achievable in thin films, making them particularly well-suited for fundamental investigations of healing phenomena prior to their translation to bulk material systems. Furthermore, the identification of mechanisms defining the healing behavior of thin metallic films may also be important for functional thin film applications for example in mechanically loaded electrical contacts, flexible electronics, thermal interface materials and stretchable sensors. That said, utilizing liquid-based self-healing mechanisms in the aforementioned application fields will require not only careful selection of the liquid phase but also further research.

Based on the classification of various self-healing mechanisms in metals by Zhang et al., the present study involves assisted self-healing based on a low-melting liquid metal that fills cracks by capillary driven infiltration [25]. In the present work, the aim is to intentionally generate damage in Al, later to be healed/filled by Sn. To this end, our work focuses on crack filling behavior using a multilayer thin film architecture as a model system for bulk, where Sn layer is directly in contact with the Al layers at the sites of damage. Specifically, we investigate the influence of annealing temperature and time on Sn mobility, with attention to the influence of crack-widths on the healing efficiency. By directly observing the crack-filling at the microscale using scanning transmission electron microscopy, this study enables a comprehensive correlation between the physical mechanisms activated during healing and their influence on the overall healing performance. Improved understanding of the underlying physical mechanisms enables future knowledge-based design of self-healing metals.

2. Materials and methods

The multilayer thin film architecture used in this study is comprised of 4 layers – Al_2O_3, Al, Sn and Al, where Al-Sn-Al constitutes the material system of interest, Al_2O_3 acts as a crack initiator for intentional damage creation to be subsequently healed by Sn, referred to as the healing agent, to heal Al, referred to as the matrix material (Fig. 1(a)). The multilayer was deposited in a lab-scale vacuum chamber with a base pressure $< 10^{-6}$ mbar by magnetron sputtering. The schematic of the deposition setup is depicted in Fig. 2. Four targets, 3 x Al and 1 x Sn, with a diameter of 50 mm were utilized for the deposition of the individual layers of the multilayer. The layers were deposited onto polished 40 x 10 x 1 mm^3 Al substrates. Aluminum was chosen as the substrate because its ductile nature enables controlled and repeatable damage generation, it is thermally stable under the applied annealing conditions, and it is compatible with the chosen material system. The substrates were mounted at a distance of 100 mm from the targets and rotated at 15 rpm for homogeneous film thickness distribution. The Al_2O_3 layer was synthesized from two Al targets using reactive pulsed magnetron sputtering in an Ar-O_2 atmosphere. The Ar and the O_2 gas flows were set to 55 and 9 sccm, respectively, resulting in a deposition pressure of 0.6 Pa. Each of the two Al targets was operated at 9.2 W cm^{-2} with a frequency of 250 kHz and a duty cycle of 60 %. The metallic layers were deposited in a pure Ar atmosphere at an Ar gas flow of 115 sccm and a corresponding pressure of 1.0 Pa in the chamber. The deposition conditions are summarized in Table 1.

Multilayer architectures with two metallic layer thicknesses were employed: 500 nm thick Al and Sn layers were initially used to determine annealing conditions to trigger Sn mobility. Subsequently, films with 1000 nm thick Al and Sn layers were utilized to investigate the effect of crack-widths on crack filling efficiency.

The as-deposited samples were bent using a 3-point bending setup in a Kammrath Weiss MB0 module to generate damage (Fig. 1(b)). By

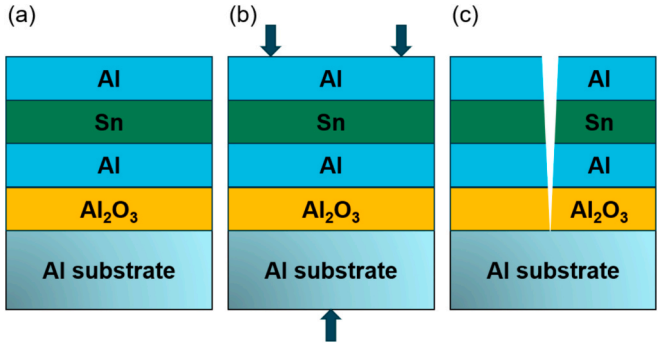

Fig. 1. (a) Schematic of the Al / Sn / Al multilayer thin film model architecture on an Al substrate. The Al_2O_3 layer is utilized as a damage formation layer. A Sn layer is encapsulated within two Al layers, mimicking a reservoir of Sn as a healing agent in the Al matrix. (b) Schematic of the bending of the as-deposited Al / Sn / Al multilayer thin film. By employing a 3-point bending module, a crack is initiated in the brittle alumina layer, which propagates to the metallic layers, creating a damaged metallic sample. (c) Schematic of a damaged sample.

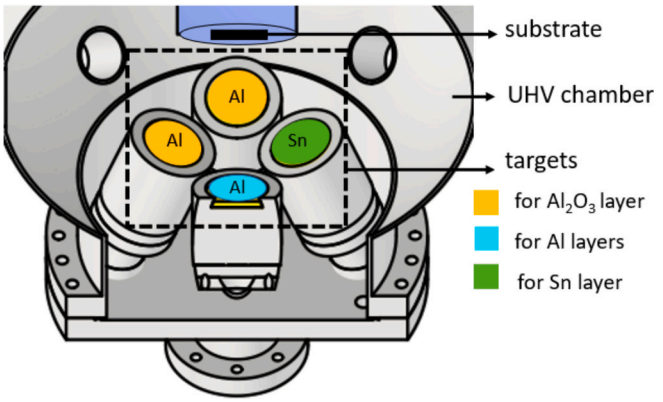

Fig. 2. Schematic of the magnetron sputtering deposition setup utilized for the deposition of the Al / Sn / Al multilayer thin film model architecture. Two Al targets (in yellow) and the one Al target (in light blue) were used for the deposition of the Al_2O_3 and of the metallic Al layers, respectively. (For interpretation of the references to colour in this figure legend, the reader is referred to the web version of this article.)

varying the relative displacement between the supporting pins and the stationary loading pin between 5–6.5 mm, the crack dimensions were varied, resulting in crack-widths between 2 and 4 μm.

The damaged samples were annealed at 250°C for 10 min and 400°C for 10 and 30 min in a pre-heated high-vacuum horizontal furnace with a base pressure ~ 10^{-6} mbar to initiate healing of the cracks in the Al layer by Sn. The cross-sections of the damaged and annealed samples were examined by lifting-out of a lamella from the cracked region, perpendicular to the crack opening, using a FEI Helios Nanolab 660 dual-beam focused ion beam (FIB) system with a Ga^+ ion source. A standard lift-out procedure was carried out to obtain the lift-out and the lamellae were thinned by a series of ion-milling steps with decreasing ion beams current until the lamella thickness was < 100 nm and attained electron transparency. A STEM detector was then used to obtain the bright field (BF) micrographs using electron beam current of 50 pA at 30 kV in field-immersion mode. Afterwards energy dispersive X-ray spectroscopy (EDX) area maps were acquired to visualize the spatial distribution of the elements and potential structure healing. An EDAX Octane Elect detector was used at 10 kV acceleration voltage and 3.2nA electron beam current.

3. Results and discussion

The as-deposited Al / Sn / Al multilayer thin film architectures were subject to bending to generate damage via the crack-initiating Al_2O_3 layer. The cracks consequently propagated to the Al and Sn layers as shown in the BF-STEM image in Fig. 3(a). The crack in the Al layer is ~ 250 nm wide. From the EDX area map shown in Fig. 3(b), it can be ascertained that the cracks in the Al layer remain unfilled in the as-damaged state. The pink regions in the EDX area maps indicate Pt originating from the liftout procedure using FIB, where Pt was deposited as protective layer on the region of interest.

The damaged samples were annealed isothermally, varying temperature and time, to identify the correlation between the mobility of the healing agent Sn and the crack healing efficiency. The BF-STEM image of the sample annealed at 250°C for 10 min can be seen in the Fig. 3(c). As opposed to the damaged sample, the Sn layer in the annealed sample appears free of cracks, further consistent with the EDX area map in Fig. 3(d). The thermal energy provided to Sn by means of the sample heating to 250°C caused melting of Sn (melting temperature, T_m = 233°C) and its localized redistribution leading to healing of the crack in the Sn layer. However, at this temperature, cracks in the Al layer remains unfilled. This behavior can be rationalized by considering the limited mobility of Sn on Al at 250°C, where Sn is wetting Al poorly, resulting in low capillary forces. Thereby, the driving force for Sn ingress into the crack is reduced, leaving the cracks in Al unfilled.

It has been shown that the contact angle of Sn on Al reduces from 116° to 30° and 11° by increasing the temperature from 350 to 400 and 450°C, respectively [26]. According to Lin et al., this reduction is partially linked to the difference in the coefficients of thermal expansion between Al and Al_2O_3, as increasing the annealing temperature causes the native Al_2O_3 to crack and debond from the underlying Al substrate, allowing Sn to permeate the oxide film and wet the Al substrate [26]. Further, it has been stated that with increasing annealing temperature, the viscosity of liquid Sn decreases [27]. Using a pre-exponential factor (A) of 0.497713 mPa.s and activation energy (E) of 5411.2 J/mol from [27], the viscosities of Sn at 250 and 400°C, as calculated in the supplementary section, are 1.734 and 1.309 mPa.s, respectively. Fig. S1 shows the decreasing trend of viscosity with temperature. The large contact angle of Sn on Al at 250°C, and the viscous resistance results in a very small capillary driving force, so that Sn does not spontaneously infiltrate and fill the crack in Al layer. Based on the temperature dependent viscosity data presented in Fig. S1, an annealing temperature of 400°C was selected, as higher temperature is expected to promote healing through a concomitant reduction in surface tension (manifested as a lower contact angle and improved wetting of Al by Sn) and a decrease in viscosity, which facilitates the flow of liquid Sn into the damaged regions.

In the sample annealed at 400°C for 10 min, similarly to the sample annealed at 250°C for 10 min, the cracks in the Sn layer were healed, and the cracks in the Al layer still remained unfilled indicative of the hindered mobility of Sn under the applied conditions, as shown in Fig. 3 (e) and (f). However, in the sample annealed at 400°C for 30 min, Fig. 3 (g) and (h), it appears that the integrity of the as-deposited multilayered structure has been disrupted, as witnessed by localized delamination. The observed structural changes in the film architecture suggest extensive interdiffusion and reorganization within the stack that happened as a consequence of longer exposure time at this temperature. The major implication of this reorganization is that Sn becomes sufficiently mobile at 400°C after 30 min and wets the Al layer. Further, from Fig. 3 (e) and (g), it can be learned that in addition to the annealing at a reasonably high temperature, the displacement of the healing agent is also time-dependent. In line with Lin et al.'s observation of debonding along the oxide Al substrate interface as a prerequisite for Sn wetting in the Al-Sn system, Eisenmenger-Sittner et al. have also emphasized the critical role of oxygen at interfaces, identifying surface oxides and interfacial impurities as potential barriers to wetting [26,28,29]. Furthermore, as the debonding of the oxide layer cannot occur instantaneously, it may contribute to the observed time-dependent mobility of Sn. Only after a

Table 1
Conditions for the deposition of an Al / Sn / Al multilayer thin film model architecture consisting of Al_2O_3, Al, Sn, and Al layers.

Nr.	Layer	Atmosphere	Pressure (Pa)	Sputtering type	Target power density (W cm^{-2})	Thickness (nm)
4	Al (top)	Ar	1.0	DC	7.6	500 or 1000
3	Sn	Ar	1.0	DC	8.0	400 or 900
					2.0	first 100
2	Al (bottom)	Ar	1.0	DC	7.6	500 or 1000
1	Al_2O_3	Ar + O_2	0.6	pulsed DC	9.2	500

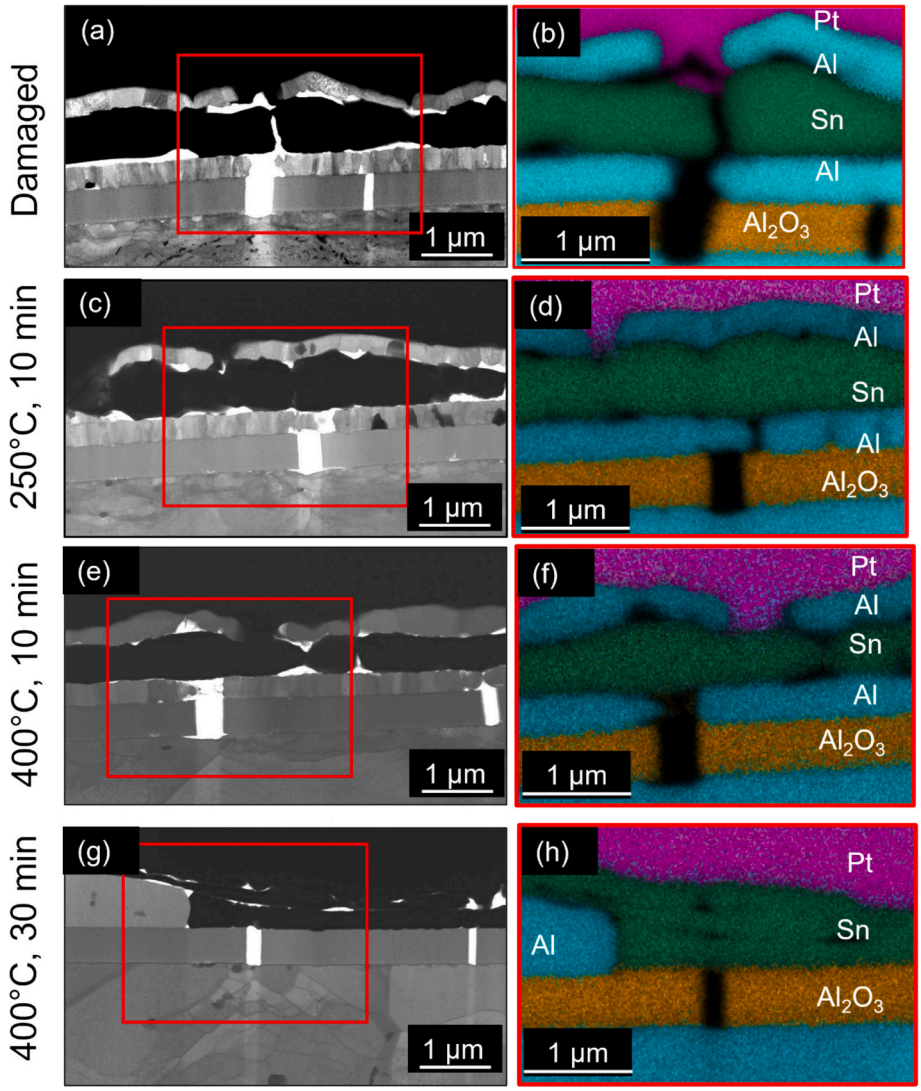

Fig. 3. BF-STEM images of lamellae lifted out from (a) damaged sample [20], (c) sample annealed at 250°C for 10 min, (e) 400°C for 10 min and (g) 400°C for 30 min with the corresponding EDX maps of the region inside the red box in (b), (d), (f) and (h), respectively. All the samples shown here possessed layers (Al, Sn, Al_2O_3) of 500 nm thickness in their as-deposited state. (For interpretation of the references to colour in this figure legend, the reader is referred to the web version of this article.)

continuous wetting Sn/Al interface is established along the crack face, can capillary-driven crack filling operate efficiently; the time required to create this pathway delays the onset of efficient crack filling. By annealing the damaged sample at 400°C for 30 min, the mobility of the healing agent Sn was successfully triggered, concurrent with the extensive reorganization of the film shown in Fig. 3(g). To preserve the integrity of the multilayer architecture during the annealing, to look past the reorganization due to the annealing conditions, and isolate the crack-filling mechanism, samples with metallic layers of double the thickness, i.e., 1000 nm-thick Al and Sn layers, were used in the subsequent experiments.

Fig. 4(a) and (b) show the damaged sample with 500 nm metallic layers as a reference, while fig. 4(c)-(h) showcase BF-STEM images and EDX maps of the cracks with different widths and annealed at 400°C for 30 min with 1000 nm thick metallic layers. From Fig. 4(c) and (d) it can be seen that Sn has diffused and filled a ~ 2.3 µm wide crack in the Al layer as opposed to the unfilled crack in the Al layer in Fig. 4(a) and (b). This observation highlights the critical role of the annealing conditions – temperature and time – on the healing process. This result aligns with the observed crack filling by Sn in thin film model systems as well as crack filling by Sn–rich eutectic (99.4 wt% Sn) in bulk Al-Sn reported in the literature [24].

However, for samples with ~ 3.5 and ~ 4.1 µm wide cracks as shown in Fig. 4(e)-(h), the cracks in the Al layers were only partially filled, although complete wetting of Al by Sn is expected at 400°C after 30 min. It is reasonable to assume that here-observed partial crack filling with increasing crack-width is due to both, a decrease in the capillary force acting on the liquid Sn and an insufficient supply of the liquid Sn for complete crack filling. This behavior is consistent with the inverse correlation between capillary force with crack width, such that the narrower cracks experiencing a higher capillary suction than wider cracks, fill more readily. Therefore, it is evident that efficient crack healing in Al by Sn requires not only external heating and time to enable wetting of Al by Sn and Sn mobility to the damage sites, but also sufficient capillary force on Sn to drive the healing action. Further, in Fig. 5(a), a cross section of a pristine sample prior to bending and annealing is shown. In the pristine sample, at the Al-Sn interface in the multilayer architecture, a few interfacial voids can be seen, likely occurring during growth. In Fig. 5(b), a BF–STEM image of an undamaged region of an annealed sample is shown. It can be observed that the interlayer bonding in the undamaged parts remains unaffected by the annealing treatment, despite presence of few sub-micrometer sized voids in the interface.

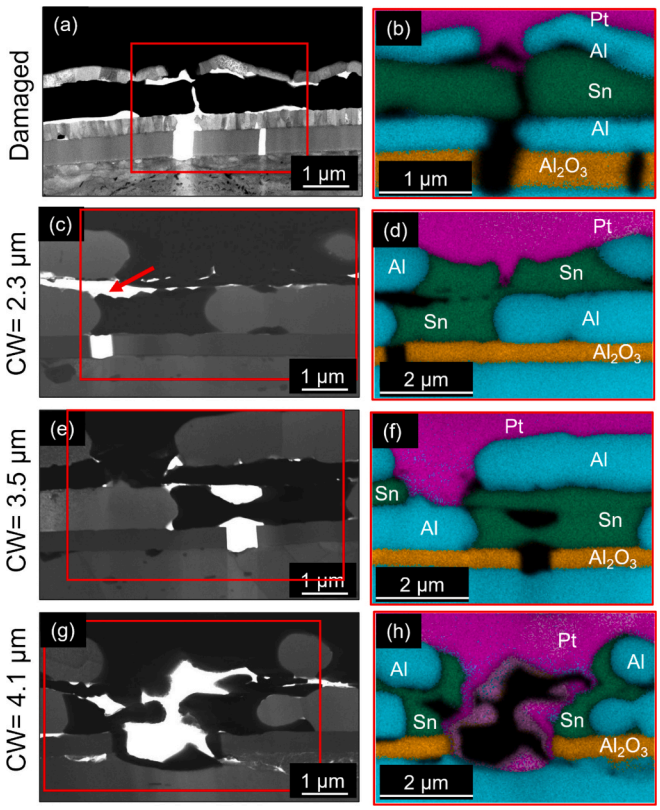

Fig. 4. BF-STEM images of the lamellae lifted out from (a) damaged sample [20], samples annealed at 400°C for 30 min with crack-widths (CW) (c) 2.3, (e) 3.5 and (g) 4.1 µm with the corresponding EDX images of the region inside the red box in (b), (d), (f), and (h), respectively. Samples shown in figures (c), (e) and (g) possessed 1000 nm thick Al and Sn layers and 500 nm thick Al_2O_3 layer in their as-deposited state, the damaged sample in figure (a) had all layers of 500 nm thickness. The red arrow in (c) points toward a void in the annealed sample. (For interpretation of the references to colour in this figure legend, the reader is referred to the web version of this article.)

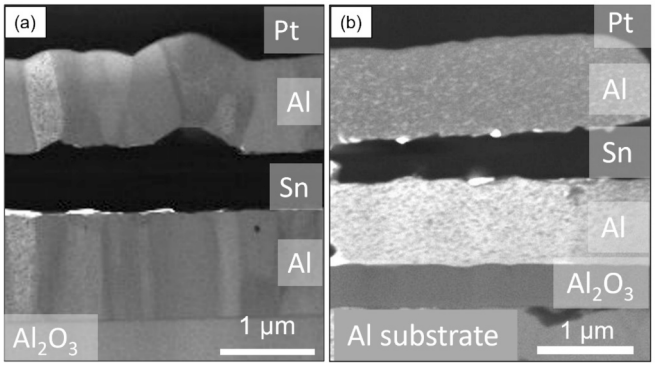

Fig. 5. BF-STEM image of (a) a pristine sample, (b) an undamaged segment from a sample with 1000 nm thick Al and Sn layers deposited on top of a 500 nm thick Al_2O_3 layer, post-annealing treatment at 400°C for 30 min.

Specifically, no evidence for delamination and/or adhesive failure can be seen. The isolated voids observed at the Al-Sn interface in the undamaged region after annealing are of the size ranging between ~ 100 nm in width and ~ 50–90 nm in height, similar to those present in the pristine multilayer. This contrasts with the micrometer sized voids with a width of ~ 2 µm and a height of ~ 300–800 nm that occur in the vicinity of the damaged regions in samples shown in Fig. 4(c)-(h). Clearly, these voids are much larger than the ones present in the pristine sample. The red arrow in Fig. 4(c) corresponds to one of the apparent voids that appear adjacent to the filled crack in the Al layer. The presence of these extended, continuous voids adjacent to the cracks or within (partially) filled cracks may arise from volume contraction during the liquid-to-solid transition of Sn, and due to the redistribution of the finite amount of healing agent into a larger cracked volume, and thus does not indicate loss of material or interfacial debonding. Additionally, Fig.S2 (b) shows oxygen map of annealed sample across the filled crack (shown in Fig. 4(e)). In the map, except for the alumina layer, no evidence for the formation of oxidized regions could be obtained. However, the oxidation of the lamella upon atmospheric exposure cannot be excluded.

The present study indicates that the mechanism of crack filling in liquid-based self-healing systems is two-step: first, thermally activated wetting of the matrix by the liquid healing agent, which requires local disruptions in the native oxides to achieve a sufficiently low contact angle; second, capillary-driven flow of the liquid into the crack volume, opposed by viscous resistance and limited by the available healing-agent reservoir. While wetting and capillary forces determine the effectiveness of the system as a self-healing material, they also define its limitations. Hence, in the above-studied system, healing was shown to be most effective in small-scale damage, an observation we expect to be relevant for other thermally-activated, liquid-based crack healing systems. Laser induced micro/nanostructuring of polyimide films, reported by Wang et al., modifies wettability of the films, so that capillary forces drive directional liquid self-transport [30]. While Wang et al.'s work shows usage of surface modification of the substrate to tailor the wetting behavior resulting in self transportation of the liquid, present work utilizes temperature dependent wetting of Al by liquid Sn to cause capillary driven motion of Sn into the crack openings, which is desirable for healing of cracks. Recently, the self-healing ability of metallic composite materials was investigated using a Bi-26In-17Sn low-melting-point (LMP) alloy as a healing agent embedded between braids made of Cu or stainless steel (SUS304) [31]. Intentional damage was introduced as cracks within the weaker LMP regions and subsequently healed by heating above the melting temperature of the LMP alloy. This work also emphasized that adequate wettability between the LMP alloy and the braid material is essential to generate sufficient capillary action for effective healing [31]. Altogether, these observations illustrate that liquid-based healing in metals is fundamentally governed by wetting-controlled capillary transport.

Sn was selected as the healing agent in this study owing to its low melting point (233°C); however, due to its intrinsically poor wetting on Al, complete crack filling of Al could only be achieved at 400°C, when annealed for 30 min. This highlights the importance of not only the low melting point but also the interfacial wettability and spreading kinetics of the healing agent on the matrix in the design of future liquid-based self-healing bulk metals and metallic thin film materials.

4. Conclusions

Due to the low melting point of Sn, the Al-Sn system is suitable for thermally activated, liquid-based self-healing. This study examines self-healing in the Al-Sn metallic system using an Al / Sn / Al multilayer thin film model architecture. Due to direct integration of Sn in the matrix, the design requirements for potential bulk manufacturing applications are simplified by avoiding ceramic encasing of Sn. The model Al / Sn / Al architecture was deposited layer-by-layer by magnetron sputtering onto an Al_2O_3 layer, introduced as a brittle layer to induce damage in the otherwise ductile metallic layers. Cracks were introduced in these model systems using a 3-point bending setup and thermal activation of the healing was achieved through annealing. After annealing at 250°C for 10 min, the cracks in the Sn layer healed via thermally induced melting and redistribution of Sn, though the effect was confined to the Sn layer due to poor wetting on Al at lower temperatures caused by their negligible mutual solubility. At 400°C, ~2 µm wide cracks in the Al layer were fully healed after 30 min, while cracks > 3 µm showed only partial

healing. Complete healing in ~ 2 μm crack at 400°C after 30 min can be attributed to the higher mobility of Sn, resulting from the improved wetting of Al by Sn at higher annealing temperature and the prolonged annealing time. The incomplete healing of > 3 μm cracks at the same annealing condition can be explained by lower capillary forces due to large crack-widths acting on the liquid Sn and/or an insufficient supply of Sn. The mobility of Sn is governed by its temperature-dependent wetting behavior and annealing time, while variations in healing efficiency are governed by the crack-width-dependent capillary forces. Despite the limitation posed by crack–width, liquid-based healing effectively fills smaller cracks in Al, ensuring complete healing for narrower cracks. Based on the understanding of wetting and capillary-driven crack filling, the future design of thermally activated liquid-based self-healing bulk metals and metallic thin films should prioritize optimizing interfacial properties between the matrix and healing agent, while selecting low-melting-point healing agents to enable effective healing.

Declaration of generative AI and AI-assisted technologies in the manuscript preparation process

During the preparation of this work the authors used OpenAI to review the language. After using this tool, the authors reviewed and edited the content as needed and take full responsibility for the content of the published article.

CRediT authorship contribution statement

Subisha Balakumar: Writing – review & editing, Writing – original draft, Visualization, Methodology, Investigation, Formal analysis, Data curation, Conceptualization. **Stanislav Mráz:** Writing – review & editing, Writing – original draft, Visualization, Methodology, Investigation, Conceptualization. **Marcus Hans:** Writing – review & editing, Methodology, Investigation, Formal analysis. **Markus Momma:** Writing – review & editing, Visualization. **Leandro Tanure:** Writing – review & editing, Conceptualization. **Hauke Springer:** Writing – review & editing, Supervision, Project administration, Funding acquisition, Conceptualization. **Jochen M. Schneider:** Writing – review & editing, Writing – original draft, Supervision, Resources, Project administration, Funding acquisition, Conceptualization.

Declaration of competing interest

The authors declare that they have no known competing financial interests or personal relationships that could have appeared to influence the work reported in this paper.

Appendix A. Supplementary data

Supplementary data to this article can be found online at https://doi.org/10.1016/j.matdes.2026.116116.

Data availability

Data will be made available on request.

References

[1] A.E. Tekkaya, P.-O. Bouchard, S. Bruschi, C.C. Tasan, Damage in metal forming, CIRP Ann. 69 (2) (Jan. 2020) 600–623, https://doi.org/10.1016/j.cirp.2020.05.005.

[2] M.A. Wollenweber, et al., On the damage behaviour in dual-phase DP800 steel deformed in single and combined strain paths, Mater. Des. 231 (Jul. 2023) 112016, https://doi.org/10.1016/j.matdes.2023.112016.

[3] S. van der Zwaag, An Introduction to Material Design Principles: Damage Prevention versus Damage Management, in: S. van der Zwaag (Ed.), Self Healing Materials: An Alternative Approach to 20 Centuries of Materials Science, Springer Netherlands, Dordrecht, 2007: pp. 1–18. https://doi.org/10.1007/978-1-4020-6250-6_1.

[4] M.D. Hager, P. Greil, C. Leyens, S. van der Zwaag, U.S. Schubert, Self-Healing Materials, Adv. Mater. 22 (2010) 5424–5430, https://doi.org/10.1002/adma.201003036.

[5] J. Dahlke, S. Zechel, M.D. Hager, U.S. Schubert, How to Design a Self-Healing Polymer: General Concepts of Dynamic Covalent Bonds and their Application for Intrinsic Healable Materials, Adv. Mater. Interfaces 5 (2018) 1800051, https://doi.org/10.1002/admi.201800051.

[6] Y. Yang, M.W. Urban, Self-Healing of Polymers via Supramolecular Chemistry, Adv. Mater. Interfaces 5 (2018) 1800384, https://doi.org/10.1002/admi.201800384.

[7] B. Grabowski, C.C. Tasan, Self-Healing Metals, in: M.D. Hager, S. van der Zwaag, U. S. Schubert (Eds.), Self-Healing Materials, Springer International Publishing, Cham, 2016: pp. 387–407. https://doi.org/10.1007/12_2015_337.

[8] N. van Dijk, S. van der Zwaag, Self-Healing Phenomena in Metals, Adv. Mater. Interfaces 5 (2018) 1800226, https://doi.org/10.1002/admi.201800226.

[9] S. Danzi, V. Schnabel, J. Gabl, A. Sologubenko, H. Galinski, R. Spolenak, Rapid On-Chip Healing of Metal Thin Films, Adv. Mater. Technol. 4 (3) (2019) 1800468, https://doi.org/10.1002/admt.201800468.

[10] C.O.W. Trost, et al., Enthalpy-Driven Self-Healing in Thin Metallic Films on Flexible Substrates, Adv. Mater. 36 (29) (2024) 2401007, https://doi.org/10.1002/adma.202401007.

[11] R.N. Lumley, I.J. Polmear, A.J. Morton, Interrupted aging and secondary precipitation in aluminium alloys, Mater. Sci. Technol. 19 (2003) 1483–1490, https://doi.org/10.1179/026708303225008112.

[12] R. Lumley, Self Healing in Aluminium Alloys, in: S. van der Zwaag (Ed.), Self Healing Materials: An Alternative Approach to 20 Centuries of Materials Science, Springer Netherlands, Dordrecht, 2007: pp. 219–254. https://doi.org/10.1007/978-1-4020-6250-6_11.

[13] N. Shinya, J. Kyono, K. Laha, Self-healing effect of Boron Nitride Precipitation on Creep Cavitation in Austenitic Stainless Steel, J. Intell. Mater. Syst. Struct. 17 (2006) 1127–1133, https://doi.org/10.1177/1045389X06065238.

[14] S. Zhang, C. Kwakernaak, W. Sloof, E. Brück, S. van der Zwaag, N. van Dijk, Self Healing of Creep damage by Gold Precipitation in Iron Alloys, Adv. Eng. Mater. 17 (2015) 598–603, https://doi.org/10.1002/adem.201400511.

[15] M.V. Manuel, G.B. Olson, Biomimetic Self-Healing Metals: Proceedings of the 1st International Conference on Self-Healing Materials, Proceedings of the 1st International Conference on Self-Healing Materials (2007).

[16] J.B. Ferguson, B.F. Schultz, P.K. Rohatgi, Zinc alloy ZA-8/shape memory alloy self-healing metal matrix composite, Mater. Sci. Eng. A 620 (2015) 85–88, https://doi.org/10.1016/j.msea.2014.10.002.

[17] M.R. Hassan, M. Mehrpouya, S. Emamian, M.N. Sheikholeslam, Review of Self-Healing effect on Shape memory Alloy (SMA) Structures, Adv. Mat. Res. 701 (2013) 87–92, https://doi.org/10.4028/www.scientific.net/AMR.701.87.

[18] J. Mohd Jani, M. Leary, A. Subic, M.A. Gibson, A review of shape memory alloy research, applications and opportunities, Materials & Design (1980-2015) 56 (2014) 1078–1113. https://doi.org/10.1016/j.matdes.2013.11.084.

[19] V. Kilicli, X. Yan, N. Salowitz, P.K. Rohatgi, Recent Advancements in Self-Healing Metallic Materials and Self-Healing Metal Matrix Composites, JOM 70 (2018) 846–854, https://doi.org/10.1007/s11837-018-2835-y.

[20] M. Nosonovsky and P. K. Rohatgi, "Introduction," in Biomimetics in Materials Science: Self-Healing, Self-Lubricating, and Self-Cleaning Materials, M. Nosonovsky and P. K. Rohatgi, Eds., New York, NY: Springer, 2012, pp. 1–22. https://doi.org/10.1007/978-1-4614-0926-7_1.

[21] J. Martinez-Lucci, R.S. Amano, P. Rohatgi, Review in self Healing in Metal Matrix Composites, Journal of Aeronautics, Astronautics and Aviation 53 (2021) 441–472, https://doi.org/10.6125/JoAAA.202112_53(4).01.

[22] J. Martínez Lucci, R.S. Amano, P.K. Rohatgi, Heat transfer and fluid flow analysis of self-healing in metallic materials, Heat Mass Transfer 53 (2017) 825–848, https://doi.org/10.1007/s00231-016-1837-y.

[23] M. Molteni, A.M. Grande, P. Bassani, E. Gariboldi, Role of microstructure in the exploitation of self-healing potential in form-stable composite phase change materials based on immiscible alloys, J. Alloy. Compd. 984 (2024) 173989, https://doi.org/10.1016/j.jallcom.2024.173989.

[24] L. Tanure, L. Patterer, S. Balakumar, M. Fekete, S. Mráz, S.K. Aghda, M. Hans, J. M. Schneider, H. Springer, A novel concept for self-healing metallic structural materials: Internal soldering of damage using low melting eutectics, Mater. Des. 252 (2025) 113821, https://doi.org/10.1016/j.matdes.2025.113821.

[25] S. Zhang, N. van Dijk, and S. van der Zwaag, "A Review of Self-healing Metals: Fundamentals, Design Principles and Performance," Acta Metall. Sin. (Engl. Lett.), vol. 33, no. 9, pp. 1167–1179, Sep. 2020, doi: 10.1007/s40195-020-01102-3.

[26] Q. Lin, W. Zhong, F. Li, W. Yu, Reactive wetting of tin/steel and tin/aluminum at 350–450 °C, J. Alloy. Compd. 716 (2017) 73–80, https://doi.org/10.1016/j.jallcom.2017.05.036.

[27] T. Gancarz, Z. Moser, W. Gąsior, J. Pstruś, H. Henein, A Comparison of Surface Tension, Viscosity, and Density of Sn and Sn–Ag Alloys using Different Measurement Techniques, Int. J. Thermophys. 32 (6) (Jun. 2011) 1210–1233, https://doi.org/10.1007/s10765-011-1011-1.

[28] C. Eisenmenger-Sittner, B. Schwarz, C. Tomastik, P.B. Barna, A. Kovacs, Experimental studies of solid state surface wetting of tin (Sn) on aluminium (Al), Appl. Surf. Sci. 252 (2006) 5466–5469, https://doi.org/10.1016/j.apsusc.2005.12.087.

[29] C. Eisenmenger-Sittner, H. Bangert, A. Bergauer, J. Brenner, H. Störi, P.B. Barna, Solid-state wetting and spreading of tin (Sn) on aluminium interfaces, Vacuum 71 (2003) 253–259, https://doi.org/10.1016/S0042-207X(02)00747-9.
[30] L. Wang, K. Yin, Q. Deng, Q. Huang, J. He, J.-A. Duan, Wetting Ridge-Guided Directional Water Self-Transport, Adv. Sci. 9 (34) (2022) 2204891, https://doi.org/10.1002/advs.202204891.
[31] S. Miyake, S. Nagahama, S. Sugano, Self-healing fiber-reinforced composite metallic material utilizing melting–solidification and capillary action, J. Mater. Res. Technol. 38 (Sep. 2025) 2480–2487, https://doi.org/10.1016/j.jmrt.2025.08.024.